Plane and Edge Point based SLAM

Sun Qinxuan

November 22, 2017

1 平面参数估计

假设待求平面参数为$(\mathbf{n}, d)$，已知平面上的点$\{\mathbf{p}_{\pi j}\}_{j=1,\cdots,N_{p\pi}}$。

1.1 不考虑测量误差

最小化点到平面的距离平方和。

$$F(\mathbf{n}, d) = \sum_{j=1}^{N_{p\pi}} D^2(\mathbf{p}_{\pi j}, \mathbf{n}, d) = \sum_{j=1}^{N_{p\pi}} \left(\mathbf{n}^T \mathbf{p}_{\pi j} + d\right)^2 \tag{1}$$

$$(\mathbf{n}^*, d^*) = \arg\min_{(\mathbf{n},d)} F(\mathbf{n}, d) \tag{2}$$

求F对d的偏导数并令其为0可得

$$d^* = -\mathbf{n}^T \mathbf{p}_G \tag{3}$$

其中$\mathbf{p}_G$是平面上点的重心位置，由式(4)计算得到。

$$\mathbf{p}_G = \frac{1}{N_{p\pi}} \sum_{j=1}^{N_{p\pi}} \mathbf{p}_{\pi j} \tag{4}$$

将式(3)代入式(1)可得

$$\begin{aligned} F(\mathbf{n}) &= \sum_{j=1}^{N_{p\pi}} \left(\mathbf{n}^T (\mathbf{p}_{\pi j} - \mathbf{p}_G)\right)^2 \\ &= \mathbf{n}^T \sum_{j=1}^{N_{p\pi}} (\mathbf{p}_{\pi j} - \mathbf{p}_G)(\mathbf{p}_{\pi j} - \mathbf{p}_G)^T \mathbf{n} \end{aligned} \tag{5}$$

令

$$\mathbf{S} = \sum_{j=1}^{N_{p\pi}} (\mathbf{p}_{\pi j} - \mathbf{p}_G)(\mathbf{p}_{\pi j} - \mathbf{p}_G)^T \tag{6}$$

则有

$$\mathbf{n}^* = \arg\min_{\mathbf{n}} \mathbf{n}^T \mathbf{S} \mathbf{n} \tag{7}$$

式(7)的解$\mathbf{n}^*$即为矩阵$\mathbf{S}$的最小特征值对应的特征向量。

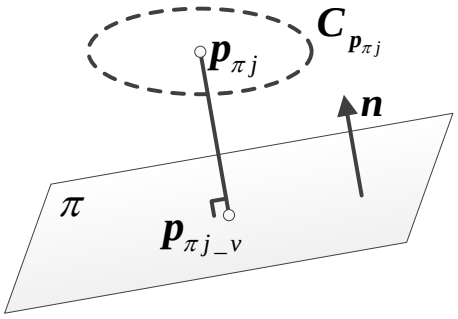

Figure 1: 考虑误差时点到平面的距离。

1.2 考虑测量误差

假设点$\mathbf{p}_{\pi j}$的测量误差可以用协方差矩阵$\mathbf{C}_{\mathbf{p}_{\pi j}}$来表示(详见1.4)。点$\mathbf{p}_{\pi j}$在平面$\pi$上的垂足为$\mathbf{p}_{\pi j_v}$。

$$\mathbf{p}_{\pi j\_v} = \mathbf{p}_{\pi j} - \left(\mathbf{n}^T \mathbf{p}_{\pi j} + d\right) \mathbf{n} \tag{8}$$

计算点$\mathbf{p}_{\pi j}$到$\mathbf{p}_{\pi j_v}$的马氏距离作为点到平面的距离$D_{w1}\left(\mathbf{p}_{\pi j}, \mathbf{n}, d\right)$，如图1所示。

$$\begin{aligned} D_{w1}^2\left(\mathbf{p}_{\pi j}, \mathbf{n}, d\right) &= \left(\mathbf{p}_{\pi j} - \mathbf{p}_{\pi j\_v}\right)^T \mathbf{C}_{\mathbf{p}_{\pi j}}^{-1} \left(\mathbf{p}_{\pi j} - \mathbf{p}_{\pi j\_v}\right) \\ &= \left(\mathbf{n}^T \mathbf{p}_{\pi j} + d\right)^2 \mathbf{n}^T \mathbf{C}_{\mathbf{p}_{\pi j}}^{-1} \mathbf{n} \end{aligned} \tag{9}$$

则

$$F_{w1}\left(\mathbf{n}, d\right) = \sum_{j=1}^{N_{p\pi}} D_{w1}^2\left(\mathbf{p}_{\pi j}, \mathbf{n}, d\right) = \sum_{j=1}^{N_{p\pi}} \left(\mathbf{n}^T \mathbf{p}_{\pi j} + d\right)^2 \mathbf{n}^T \mathbf{C}_{\mathbf{p}_{\pi j}}^{-1} \mathbf{n} \tag{10}$$

$$\left(\mathbf{n}^*, d^*\right) = \arg\min_{(\mathbf{n}, d)} F_{w1}\left(\mathbf{n}, d\right) \tag{11}$$

求F对d的偏导数并令其为0可得

$$d^* = -\mathbf{n}^T \mathbf{p}_{Gw1}\left(\mathbf{n}\right) \tag{12}$$

其中

$$\mathbf{p}_{Gw1}\left(\mathbf{n}\right) = \frac{\sum_{j=1}^{N_{p\pi}} \mathbf{n}^T \mathbf{C}_{\mathbf{p}_{\pi j}}^{-1} \mathbf{n} \mathbf{p}_{\pi j}}{\sum_{j=1}^{N_{p\pi}} \mathbf{n}^T \mathbf{C}_{\mathbf{p}_{\pi j}}^{-1} \mathbf{n}} \tag{13}$$

将式(12)代入(10)可得

$$\begin{aligned} F_{w1}\left(\mathbf{n}\right) &= \sum_{j=1}^{N_{p\pi}} \left(\mathbf{n}^T \left(\mathbf{p}_{\pi j} - \mathbf{p}_{Gw}\left(\mathbf{n}\right)\right)\right)^2 \mathbf{n}^T \mathbf{C}_{\mathbf{p}_{\pi j}}^{-1} \mathbf{n} \\ &= \mathbf{n}^T \sum_{j=1}^{N_{p\pi}} \left(\mathbf{p}_{\pi j} - \mathbf{p}_{Gw}\left(\mathbf{n}\right)\right) \mathbf{n}^T \mathbf{C}_{\mathbf{p}_{\pi j}}^{-1} \mathbf{n} \left(\mathbf{p}_{\pi j} - \mathbf{p}_{Gw}\left(\mathbf{n}\right)\right)^T \mathbf{n} \end{aligned} \tag{14}$$

则考虑测量误差时的平面法向量$\mathbf{n}$可通过最小化$F_{w1}\left(\mathbf{n}\right)$来得到。

$$\mathbf{n}^* = \arg\min_{\mathbf{n}} F_{w1}\left(\mathbf{n}\right) \tag{15}$$

但是由于式(15)不存在解析解，所以需要进行数值迭代求解的过程。注意到式(13)和式(14) 中的一项$\mathbf{n}^T \mathbf{C}_{\mathbf{p}_{\pi j}}^{-1} \mathbf{n}$，这一项表示点$\mathbf{p}_{\pi j}$的协方差矩阵$\mathbf{C}_{\mathbf{p}_{\pi j}}^{-1}$在平面法向量$\mathbf{n}$方向上

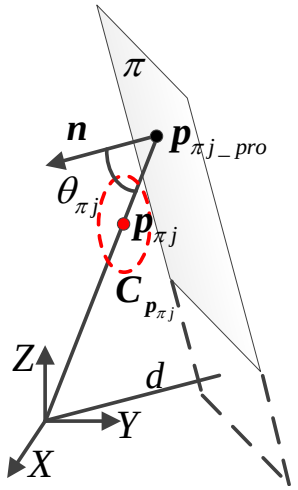

Figure 2: 考虑误差以及入射角时点到平面的距离。

的投影。在这里做一个近似，令$\mathbf{n}=\hat{\mathbf{n}}$，$\hat{\mathbf{n}}$表示式(7)的解，即不考虑测量误差时的法向量估计结果。这时有$\mathbf{p}_{Gw1}(\mathbf{n})=\mathbf{p}_{Gw1}(\hat{\mathbf{n}})$，令

$$\mathbf{S}_{w1}=\sum_{j=1}^{N_{p\pi}}\left(\mathbf{p}_{\pi j}-\mathbf{p}_{Gw1}(\hat{\mathbf{n}})\right)\hat{\mathbf{n}}^T\mathbf{C}_{\mathbf{p}_{\pi j}}^{-1}\hat{\mathbf{n}}\left(\mathbf{p}_{\pi j}-\mathbf{p}_{Gw1}(\hat{\mathbf{n}})\right)^T \tag{16}$$

则有

$$\mathbf{n}^*=\arg\min_{\mathbf{n}}\mathbf{n}^T\mathbf{S}_{w1}\mathbf{n} \tag{17}$$

式(17)的解$\mathbf{n}^*$即为矩阵$\mathbf{S}_{w1}$的最小特征值对应的特征向量。

1.3 考虑测量误差以及入射角

假设点$\mathbf{p}_{\pi j}$的测量误差可以用协方差矩阵$\mathbf{C}_{\mathbf{p}_{\pi j}}$来表示(详见1.4)。由坐标系原点到$\mathbf{p}_{\pi j}$的射线与平面$\pi$的交点为$\mathbf{p}_{\pi j_pro}$，如图2 所示。

$$\mathbf{p}_{\pi j\_pro}=\frac{-d}{\mathbf{n}^T\mathbf{p}_{\pi j}}\mathbf{p}_{\pi j} \tag{18}$$

计算点$\mathbf{p}_{\pi j}$到$\mathbf{p}_{\pi j_pro}$的马氏距离作为点到平面的距离$D_{w2}(\mathbf{p}_{\pi j},\mathbf{n},d)$。

$$\begin{aligned}D_{w2}^2(\mathbf{p}_{\pi j},\mathbf{n},d)&=\left(\mathbf{p}_{\pi j}-\mathbf{p}_{\pi j\_pro}\right)^T\mathbf{C}_{\mathbf{p}_{\pi j}}^{-1}\left(\mathbf{p}_{\pi j}-\mathbf{p}_{\pi j\_pro}\right)\\&=\left(\mathbf{n}^T\mathbf{p}_{\pi j}+d\right)^2\frac{\mathbf{p}_{\pi j}^T}{\mathbf{n}^T\mathbf{p}_{\pi j}}\mathbf{C}_{\mathbf{p}_{\pi j}}^{-1}\frac{\mathbf{p}_{\pi j}}{\mathbf{n}^T\mathbf{p}_{\pi j}}\end{aligned} \tag{19}$$

令

$$c_j(\mathbf{n})=\frac{\mathbf{p}_{\pi j}^T}{\mathbf{n}^T\mathbf{p}_{\pi j}}\mathbf{C}_{\mathbf{p}_{\pi j}}^{-1}\frac{\mathbf{p}_{\pi j}}{\mathbf{n}^T\mathbf{p}_{\pi j}} \tag{20}$$

考虑$c_j(\mathbf{n})$中各项，向量$\frac{\mathbf{p}_{\pi j}^T}{\mathbf{n}^T\mathbf{p}_{\pi j}}$的方向即为向量$\mathbf{p}_{\pi j}$的方向，设其方向的单位向量为$\mathbf{v}_{\mathbf{p}_{\pi j}}$，其幅值为

$$\left|\frac{\mathbf{p}_{\pi j}^T}{\mathbf{n}^T\mathbf{p}_{\pi j}}\right|=\frac{1}{\cos\theta_{\pi j}} \tag{21}$$

其中$\theta_{\pi j} \in [0, \frac{\pi}{2})$为向量$\mathbf{p}_{\pi j}$向平面$\pi$的入射角，如图2中所示。则有

$$c_j(\mathbf{n}) = \frac{1}{\cos^2\theta_{\pi j}} \mathbf{v}_{\mathbf{p}_{\pi j}}^T \mathbf{C}_{\mathbf{p}_{\pi j}}^{-1} \mathbf{v}_{\mathbf{p}_{\pi j}} \tag{22}$$

其中$\mathbf{v}_{\mathbf{p}_{\pi j}}^T \mathbf{C}_{\mathbf{p}_{\pi j}}^{-1} \mathbf{v}_{\mathbf{p}_{\pi j}}$即为协方差矩阵在$\mathbf{v}_{\mathbf{p}_{\pi j}}$方向的分量，而$\frac{1}{\cos^2\theta_{\pi j}}$这一项与入射角$\theta_{\pi j}$相关，$\theta_{\pi j}$越大，$c_j(\mathbf{n})$越大，则距离$D_{w2}(\mathbf{p}_{\pi j}, \mathbf{n}, d)$也越大。同样的，这里做一个近似，令$\mathbf{n} = \hat{\mathbf{n}}$，$\hat{\mathbf{n}}$表示式(7)的解，这时有$c_j(\mathbf{n}) = c_j(\hat{\mathbf{n}})$。则

$$F_{w2}(\mathbf{n}, d) = \sum_{j=1}^{N_{p\pi}} D_{w2}^2(\mathbf{p}_{\pi j}, \mathbf{n}, d) = \sum_{j=1}^{N_{p\pi}} c_j(\hat{\mathbf{n}}) \left(\mathbf{n}^T \mathbf{p}_{\pi j} + d\right)^2 \tag{23}$$

$$(\mathbf{n}^*, d^*) = \arg\min_{(\mathbf{n}, d)} F_{w2}(\mathbf{n}, d) \tag{24}$$

求F_{w2}对d的偏导数并令其为0可得

$$d^* = -\mathbf{n}^T \mathbf{p}_{Gw2}(\hat{\mathbf{n}}) \tag{25}$$

其中

$$\mathbf{p}_{Gw2}(\hat{\mathbf{n}}) = \frac{\sum_{j=1}^{N_{p\pi}} c_j(\hat{\mathbf{n}}) \mathbf{p}_{\pi j}}{\sum_{j=1}^{N_{p\pi}} c_j(\hat{\mathbf{n}})} \tag{26}$$

将式(25)代入(23)可得

$$\begin{aligned} F_{w2}(\mathbf{n}) &= \sum_{j=1}^{N_{p\pi}} c_j(\hat{\mathbf{n}}) \left(\mathbf{n}^T (\mathbf{p}_{\pi j} - \mathbf{p}_{Gw2}(\hat{\mathbf{n}}))\right)^2 \\ &= \mathbf{n}^T \sum_{j=1}^{N_{p\pi}} c_j(\hat{\mathbf{n}}) (\mathbf{p}_{\pi j} - \mathbf{p}_{Gw2}(\hat{\mathbf{n}})) (\mathbf{p}_{\pi j} - \mathbf{p}_{Gw2}(\hat{\mathbf{n}}))^T \mathbf{n} \quad = \mathbf{n}^T \mathbf{S}_{w2} \mathbf{n} \end{aligned} \tag{27}$$

则有

$$\mathbf{n}^* = \arg\min_{\mathbf{n}} \mathbf{n}^T \mathbf{S}_{w2} \mathbf{n} \tag{28}$$

式(28)的解$\mathbf{n}^*$即为矩阵$\mathbf{S}_{w2}$的最小特征值对应的特征向量。

1.4 测量误差的计算

由文献[3]中的Kinect传感器误差模型可知，深度测量误差的标准差为

2 基于平面和边缘点的机器人位姿估计

假设连续两帧(当前帧和参考帧)之间有N_π对匹配平面(平面间对应关系的建立请见xx)，$\{{}^c\pi_i, {}^r\pi_i\}_{i=1,\cdots,N_\pi}$，$\mathbf{w} = [\mathbf{t}^T, \omega^T]^T$表示两帧之间的六自由度(6-DoF)三维坐标变换。

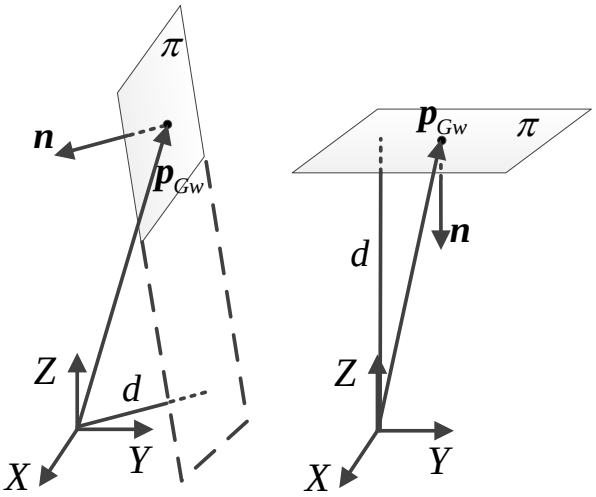

Figure 3: α_d较小(左)与α_d较大(右)时平面位姿示意图。

右下标i	平面下标;
右下标k	边缘点下标;
左上标c	当前帧;
左上标r	参考帧;
$\{{}^c\pi_i, {}^r\pi_i\}_{i=1,\cdots,N_\pi}$	两帧之间的对应平面;
$\{{}^c\mathbf{p}_{ok}, {}^r\mathbf{p}_{ok}\}_{k=1,\cdots,N_p}$	两帧之间的对应边缘点;
$\mathbf{w} = [\mathbf{t}^T, \omega^T]^T \in \mathbb{R}^6$	6-DoF位姿变换;
$T_{cr} \in \mathbb{SE}(3)$	参考帧到当前帧的变换矩阵;

2.1 平面参数对位姿估计的约束分析

定义目标函数为

$$\begin{aligned} J_\pi(\mathbf{w}) &= \sum_{i=1}^{N} J_{\pi i}(\mathbf{w}) \\ J_{\pi i}(\mathbf{w}) &= \left\| {}^c\mathbf{n}_i - \mathbf{R}_{cr}\, {}^r\mathbf{n}_i \right\|_2^2 + \left({}^cd_i - \left({}^rd_i + {}^c\mathbf{n}_i^T \mathbf{t}_{cr} \right) \right)^2 \end{aligned} \tag{29}$$

The matrix $\mathbf{\Psi}_\pi$ is calculated by

$$\begin{aligned} \mathbf{\Psi}_\pi &= \sum_{i=1}^{N} \left(\frac{\partial J_{\pi i}}{\partial \mathbf{w}} \right) \left(\frac{\partial J_{\pi i}}{\partial \mathbf{w}} \right)^T \\ &= \sum_{i=1}^{N} 4 \begin{bmatrix} \left({}^rd_i - {}^cd_i \right)^2 {}^c\mathbf{n}_i {}^c\mathbf{n}_i^T & \mathbf{0}_{3\times 3} \\ \mathbf{0}_{3\times 3} & \left({}^c\mathbf{n}_i \times {}^r\mathbf{n}_i \right) \left({}^c\mathbf{n}_i \times {}^r\mathbf{n}_i \right)^T \end{bmatrix} \end{aligned} \tag{30}$$

The matrix $\mathbf{\Psi}_\pi$ is actually a scatter matrix which contains information about the distribution of the gradient of $J_{\pi,i}$ w.r.t. $\mathbf{w}$ over all planes in the matched plane set. Performing principal component analysis upon $\mathbf{\Psi}_\pi$ results in

$$\mathbf{\Psi}_\pi = Q_\pi \Lambda_\pi Q_\pi^T = \begin{bmatrix} \mathbf{q}_{\pi 1} & \cdots & \mathbf{q}_{\pi 6} \end{bmatrix} \begin{bmatrix} \lambda_{\pi 1} & & \\ & \ddots & \\ & & \lambda_{\pi 6} \end{bmatrix} \begin{bmatrix} \mathbf{q}_{\pi 1}^T \\ \vdots \\ \mathbf{q}_{\pi 6}^T \end{bmatrix} \tag{31}$$

where $\lambda_1 \geq \lambda_2 \geq \cdots \geq \lambda_6$ are the eigenvalues of Ψ_π, and $\mathbf{q}_i$ are the corresponding eigenvectors, of which the first three elements are the translation components, and the last three elements are the rotation components. The eigenvector $\mathbf{q}_1$ corresponding to the largest eigenvalue represents the transformation of maximum constraint. Perturbing the plane parameters by the transformation of the direction $\mathbf{q}_1$ will result in the largest possible change in from among all possible transformation perturbations.

2.1.1 Degenerate Cases

Define the matrix $\mathbf{H}$ and compute its SVD decomposition as

$$\mathbf{H} = \sum_{i=1}^{N} {}^r\mathbf{n}_i {}^c\mathbf{n}_i^T = \mathbf{U}_\pi \mathbf{\Lambda}_\pi \mathbf{V}_\pi^T = \lambda_{\pi,1}\mathbf{u}_{\pi,1}\mathbf{v}_{\pi,1}^T + \lambda_{\pi,2}\mathbf{u}_{\pi,2}\mathbf{v}_{\pi,2}^T + \lambda_{\pi,3}\mathbf{u}_{\pi,3}\mathbf{v}_{\pi,3}^T \tag{32}$$

where the singular values $\lambda_{\pi,1}, \lambda_{\pi,2}, \lambda_{\pi,3}$ satisfy $\lambda_{\pi,1} \geq \lambda_{\pi,2} \geq \lambda_{\pi,3}$.

(1) Assuming that $\lambda_{\pi,3} = 0$, ${}^c\mathbf{n}_i^T\mathbf{v}_{\pi,3} = 0$ holds true for all $i = 1, \cdots, N$. For a small camera motion $\delta\mathbf{w} = [\mu\mathbf{v}_{\pi,3}^T, \mathbf{0}^T]^T$ in the direction of $\mathbf{v}_{\pi,3}$, the variation of the cost function $\delta J_\pi(\delta\mathbf{w}) = \delta\mathbf{w}^T\mathbf{\Psi}_\pi\delta\mathbf{w}$ caused by $\delta\mathbf{w}$ is always zero. That is to say, the perturbation in the direction of $\mathbf{v}_{\pi,3}$ will cause no change of the cost function.

(2) Similarly, when $\lambda_{\pi,1} = \lambda_{\pi,2} = 0$, for all $i = 1, \cdots, N$ ${}^c\mathbf{n}_i$ satisfies ${}^c\mathbf{n}_i^T\mathbf{v}_{\pi,2} = 0$, ${}^c\mathbf{n}_i^T\mathbf{v}_{\pi,3} = 0$ and ${}^c\mathbf{n}_i \times \mathbf{v}_{\pi,1} = 0$. In this case, for a small camera motion $\delta\mathbf{w} = [\mu_1\mathbf{v}_{\pi,2}^T + \mu_2\mathbf{v}_{\pi,3}^T, \mu_3\mathbf{v}_{\pi,1}^T]^T$, $\delta J_\pi(\delta\mathbf{w}) = 0$.

2.2 边缘点对位姿估计的约束分析

2.3 基于平面和边缘点的机器人位姿估计

2.4 Edge-based Camera Motion Estimation

2.4.1 Points' Constraints on Camera Motion

Suppose that all the occluding edge points are directly used in the pose estimation.

$$\begin{aligned} J_p(\mathbf{w}) &= \sum_{k=1}^{N_p} J_{p,k} = \sum_{k=1}^{N_p} \mathbf{e}_k^T\mathbf{e}_k \\ &= \sum_{k=1}^{N_p} \left({}^c\mathbf{p}'_{o,k} - R_{cr}\left({}^r\mathbf{p}'_{o,k}\right) - \mathbf{t}'_{cr}\right)^T \left({}^c\mathbf{p}'_{o,k} - R_{cr}\left({}^r\mathbf{p}'_{o,k}\right) - \mathbf{t}'_{cr}\right)) \end{aligned} \tag{33}$$

where all the point coordinates are referred to the centroid.

$$\begin{aligned} &\mathbf{t}'_{cr} = \mathbf{t}_{cr} - {}^c\bar{\mathbf{p}}_o + R_{cr}({}^r\bar{\mathbf{p}}_o) \\ &{}^c\mathbf{p}'_{o,k} = {}^c\mathbf{p}_{o,k} - {}^c\bar{\mathbf{p}}_o,\ {}^r\mathbf{p}'_{o,k} = {}^r\mathbf{p}_{o,k} - {}^r\bar{\mathbf{p}}_o \\ &{}^c\bar{\mathbf{p}}_o = \frac{1}{N_p}\sum_{k=1}^{N_p} {}^c\mathbf{p}_{o,k},\ {}^r\bar{\mathbf{p}}_o = \frac{1}{N_p}\sum_{k=1}^{N_p} {}^r\mathbf{p}_{o,k} \end{aligned} \tag{34}$$

The scatter matrix $\mathbf{\Psi}_p$ is defined likewise.

$$\mathbf{\Psi}_p = \sum_{k=1}^{N_p} \left(\frac{\partial J_{p,k}}{\partial \mathbf{w}} \right) \left(\frac{\partial J_{p,k}}{\partial \mathbf{w}} \right)^T \tag{35}$$

where

$$\frac{\partial J_{p,k}}{\partial \mathbf{w}} = -2 \begin{bmatrix} \mathbf{I}_{3\times 3} \\ {}^r\hat{\mathbf{p}}'_{o,k} \end{bmatrix} \left({}^c\mathbf{p}'_{o,k} - R_{cr}({}^r\mathbf{p}'_{o,k}) - \mathbf{t}_{cr} \right) \tag{36}$$

2.4.2 Degenerate Cases

(1) It can be seen from $\mathbf{\Psi}_p$ that if $\exists \mathbf{v}$ such that ${}^r\mathbf{p}'_{o,k} \times \mathbf{v} = 0$ for all $k = 1, \cdots, N_p$, i.e., the measured points are collinear (at least two points), $\delta J_p(\delta\mathbf{w}) = \delta\mathbf{w}^T \mathbf{\Psi}_p \delta\mathbf{w} = 0$ for $\delta\mathbf{w} = [\mathbf{0}^T, \mu\mathbf{v}^T]^T$.

(2) If there is only one measured point, ${}^r\mathbf{p}'_{o,k} = \mathbf{0}$. In this case, for any rotation $\omega \in \mathbb{R}^3$, $\delta J_p(\delta\mathbf{w}) = \delta\mathbf{w}^T \mathbf{\Psi}_p \delta\mathbf{w} = 0$ for $\delta\mathbf{w} = [\mathbf{0}^T, \omega^T]^T$.

2.5 Plane-Edge-based Camera Motion Estimation

The overall objective function is

$$J(\mathbf{w}) = J_\pi(\mathbf{w}) + J_{pw}(\mathbf{w}) \tag{37}$$

2.5.1 Point Weighting

For each occluding edge point ${}^c\mathbf{p}_{o,k}$, a weight $\alpha_{p,k}$ is assigned to the corresponding component in the cost function

$$J_{pw}(\mathbf{w}) = \sum_{k=1}^{N_p} \alpha_{p,k} J_{p,k} \tag{38}$$

$$\alpha_{p,k} = \frac{\left(\frac{\partial J_{p,k}}{\partial \mathbf{w}} \right)^T \mathbf{q}_{\pi,j}}{\left| \frac{\partial J_{p,k}}{\partial \mathbf{w}} \right| \sqrt{\frac{\lambda_{\pi,j}}{\bar{\lambda}_\pi}}} \tag{39}$$

$$j = \arg\max_j \frac{\left(\frac{\partial J_{p,k}}{\partial \mathbf{w}} \right)^T \mathbf{q}_{\pi,j}}{\left| \frac{\partial J_{p,k}}{\partial \mathbf{w}} \right|} \tag{40}$$

$$\bar{\lambda}_\pi = \frac{1}{6} \sum_{t=1}^{6} \lambda_{\pi,t} \tag{41}$$

2.5.2 Degenerate Cases

Suppose that the measurements include both planes and points. Combining the degenerate cases stated in 1.1.2 and 1.2.2 yields the following cases.

(1) $\lambda_{\pi,1} = \lambda_{\pi,2} = 0$ and ${}^r\mathbf{p}'_{o,k} \times \mathbf{v} = 0$ for all $k = 1, \cdots, N_p$ hold true simultaneously, and $\mathbf{v}$ and $\mathbf{v}_{\pi,1}$ happen to be of the same direction, i.e., $\mathbf{v} \times \mathbf{v}_{\pi,1} = 0$. In this case, the camera motion along $\delta\mathbf{w} = [\mathbf{0}^T, \mu\mathbf{v}_{\pi,1}^T]^T$ cannot be constrained.

(2) If $\lambda_{\pi,1} = \lambda_{\pi,2} = 0$ and there is only one measured point, the camera motion along $\delta\mathbf{w} = [\mathbf{0}^T, \mu\mathbf{v}_{\pi,1}^T]^T$ cannot be constrained.

3 Plane and Point based Camera Tracking with Unknown Correspondences

The plane segmentation method proposed in [1] and the edge detection method proposed in [2] are used to detect the planar segments and edge points in an RGB-D scan.

A detected planar segment $\mathcal{P}_i, i = 1, \cdots, N$ has the following attributes.

- plane parameters $\pi_i = [\mathbf{n}_i^T, d_i]^T$
- number of points $N_{\pi,i}$
- centroid $\mathbf{p}_{\pi,i}$
- covariance $\mathbf{C}_{\pi,i}$

Suppose that $\{{}^r\mathcal{P}_i\}_{i=1,\cdots,N_r}$ and $\{{}^c\mathcal{P}_j\}_{j=1,\cdots,N_c}$ are planar segments extracted from reference and current frame, respectively. Each planar segment $\mathcal{P}_i$ is modeled as a Gaussian distribution $\mathcal{N}(\mathbf{p}_{\pi,i}, \mathbf{C}_{\pi,i})$. $\{{}^r\mathbf{p}_{o,k}\}_{k=1,\cdots,N_{pr}}$ and $\{{}^c\mathbf{p}_{o,l}\}_{l=1,\cdots,N_{pc}}$ are occluding edge points extracted from reference and current frame, respectively. The planar segments and occluding edge points extracted from two successive frames are used simultaneously in a ICP framework. In each iteration of ICP, the correspondences between planar segments are assigned by checking the Bhattacharyya distance between the Gaussian distribution that models the planar segments.

$$D_{Bha}(\mathcal{P}_i, \mathcal{P}_j) = \frac{1}{8}(\mathbf{p}_{\pi,i} - \mathbf{p}_{\pi,j})^T \mathbf{C}_\pi^{-1} (\mathbf{p}_{\pi,i} - \mathbf{p}_{\pi,j}) + \frac{1}{2}\ln\left(\frac{|\mathbf{C}_\pi|}{\sqrt{|\mathbf{C}_{\pi,i}||\mathbf{C}_{\pi,j}|}}\right) \tag{42}$$

where $\mathbf{C}_\pi = \frac{1}{2}(\mathbf{C}_{\pi,i} + \mathbf{C}_{\pi,j})$. The correspondences between points are assigned by checking the Euclidean distance between the point coordinates.

$$D_{Euc}(\mathbf{p}_{o,k}, \mathbf{p}_{o,l}) = \|\mathbf{p}_{o,k} - \mathbf{p}_{o,l}\|_2 \tag{43}$$

The whole ICP framework is presented in Algorithm 2.

Algorithm 1 Planar Segment and Occluding Edge Point based ICP

Inputs:

Planar segments extracted from two frames $\{{}^r\mathcal{P}_i\}_{i=1,\cdots,N_r}$ and $\{{}^c\mathcal{P}_j\}_{j=1,\cdots,N_c}$.

Occluding edge points extracted from two frames $\{{}^r\mathbf{p}_{o,k}\}_{k=1,\cdots,N_{pr}}$ and $\{{}^c\mathbf{p}_{o,l}\}_{l=1,\cdots,N_{pc}}$.

Outputs:

Transformation between two frames $T_{cr} = \mathbf{R}_{cr}, \mathbf{t}_{cr}$.

4 Plane Fusion

A plane $\mathcal{P}_i$

Table 1:

	Plane-Point ICP	STING
Fr1/xyz	0.0123	**0.0114**
Fr1/room	**0.0817**	0.0832
Fr3/cabinet	0.0382	**0.0326**

- plane parameters $\pi_i = [\mathbf{n}_i^T, d_i]^T$
- number of points $N_{\pi,i}$
- centroid $\mathbf{p}_{\pi,i}$
- covariance $\mathbf{C}_{\pi,i}$
- curvature $\rho_{\pi,i}$ [1]
- shadow points $\left\{\mathbf{p}_{s,k}^i, k = 1, \cdots, N_p^i\right\}$

5 Least Primitives for Pose Estimation

5.1 Three Planes

Three corresponding non-parallel planes $\{{}^r\pi_i, {}^c\pi_i, \}_{i=1,2,3}$. Let

$$\begin{aligned} {}^r\mathbf{M}_1 &= \begin{bmatrix} {}^r\mathbf{n}_1 & {}^r\mathbf{n}_2 & {}^r\mathbf{n}_3 \end{bmatrix} \\ {}^c\mathbf{M}_1 &= \begin{bmatrix} {}^c\mathbf{n}_1 & {}^c\mathbf{n}_2 & {}^c\mathbf{n}_3 \end{bmatrix} \\ \mathbf{d} &= \begin{bmatrix} {}^cd_1 - {}^rd_1 \\ {}^cd_2 - {}^rd_2 \\ {}^cd_3 - {}^rd_3 \end{bmatrix} \end{aligned} \tag{44}$$

The rotation $\mathbf{R}_{cr}$ and translation $\mathbf{t}_{cr}$ can be computed as

$$\begin{aligned} \mathbf{R}_{cr} &= {}^c\mathbf{M}_1 {}^r\mathbf{M}_1^{-1} \\ \mathbf{t}_{cr} &= {}^c\mathbf{M}_1^{-T}\mathbf{d} \end{aligned} \tag{45}$$

5.2 Two Planes and One Point

Two corresponding non-parallel planes $\{{}^r\pi_i, {}^c\pi_i, \}_{i=1,2}$ and one corresponding point $\{{}^r\mathbf{p}_o, {}^c\mathbf{p}_o\}$. Construct three axes ${}^r\hat{\mathbf{x}}, {}^r\hat{\mathbf{y}}, {}^r\hat{\mathbf{z}}$ in reference coordinate system and locate the origin at ${}^r\mathbf{p}_o$.

$$\begin{aligned} {}^r\hat{\mathbf{x}} &= -{}^r\mathbf{n}_2 \\ {}^r\hat{\mathbf{y}} &= {}^r\mathbf{n}_1 \times {}^r\mathbf{n}_2 \\ {}^r\hat{\mathbf{z}} &= {}^r\hat{\mathbf{x}} \times {}^r\hat{\mathbf{y}} \end{aligned} \tag{46}$$

[1] Note that the curvature here is just an indication that tells how a surface deviates from being a flat plane, rather than the strictly defined curvature.

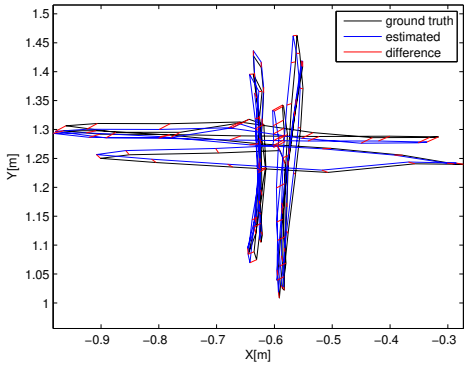

(a)

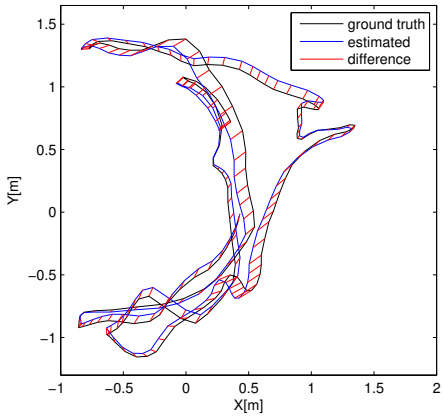

(b)

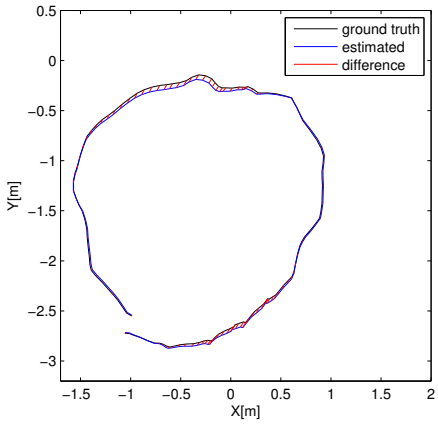

(c)

Figure 4: (a)Fr1/xyz; (b)Fr1/room; (c)Fr3/cabinet;

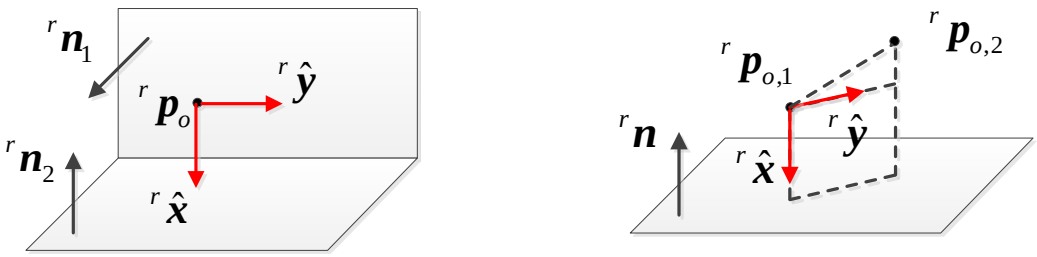

(a) (b)

Figure 5:

The axes and the origin in current frame is constructed likewise.

$$\begin{aligned} {}^c\hat{\mathbf{x}} &= -{}^c\mathbf{n}_2 \\ {}^c\hat{\mathbf{y}} &= {}^c\mathbf{n}_1 \times {}^c\mathbf{n}_2 \\ {}^c\hat{\mathbf{z}} &= {}^c\hat{\mathbf{x}} \times {}^c\hat{\mathbf{y}} \end{aligned} \tag{47}$$

Let

$$\begin{aligned} {}^r\mathbf{M}_2 &= \begin{bmatrix} {}^r\hat{\mathbf{x}} & {}^r\hat{\mathbf{y}} & {}^r\hat{\mathbf{z}} \end{bmatrix} \\ {}^c\mathbf{M}_2 &= \begin{bmatrix} {}^c\hat{\mathbf{x}} & {}^c\hat{\mathbf{y}} & {}^c\hat{\mathbf{z}} \end{bmatrix} \end{aligned} \tag{48}$$

Then the rotation $\mathbf{R}_{cr}$ and translation $\mathbf{t}_{cr}$ can be computed as

$$\begin{aligned} \mathbf{R}_{cr} &= {}^c\mathbf{M}_2 {}^r\mathbf{M}_2^T \\ \mathbf{t}_{cr} &= {}^c\mathbf{p}_o - \mathbf{R}_{cr} {}^r\mathbf{p}_o \end{aligned} \tag{49}$$

5.3 One Plane and Two Points

One corresponding plane $\{{}^r\pi, {}^c\pi, \}$ and two different corresponding points $\{{}^r\mathbf{p}_{o,j}, {}^c\mathbf{p}_{o,j}\}_{j=1,2}$ satisfying $({}^r\mathbf{p}_{o,1} - {}^r\mathbf{p}_{o,2}) \times {}^r\mathbf{n} \neq 0$ and $({}^c\mathbf{p}_{o,1} - {}^c\mathbf{p}_{o,2}) \times {}^c\mathbf{n} \neq 0$. Construct three axes ${}^r\hat{\mathbf{x}}, {}^r\hat{\mathbf{y}}, {}^r\hat{\mathbf{z}}$ in reference coordinate system and locate the origin at ${}^r\mathbf{p}_{o,1}$.

$$\begin{aligned} {}^r\hat{\mathbf{x}} &= -{}^r\mathbf{n} \\ {}^r\mathbf{y} &= ({}^r\mathbf{p}_{o,2} - {}^r\mathbf{p}_{o,1}) - \left(({}^r\mathbf{p}_{o,2} - {}^r\mathbf{p}_{o,1})^T {}^r\mathbf{n} \right) {}^r\mathbf{n} \\ {}^r\hat{\mathbf{y}} &= \frac{{}^r\mathbf{y}}{\|{}^r\mathbf{y}\|} \\ {}^r\hat{\mathbf{z}} &= {}^r\hat{\mathbf{x}} \times {}^r\hat{\mathbf{y}} \end{aligned} \tag{50}$$

The axes and the origin in current frame is constructed likewise.

$$\begin{aligned} {}^c\hat{\mathbf{x}} &= -{}^c\mathbf{n} \\ {}^c\mathbf{y} &= ({}^c\mathbf{p}_{o,2} - {}^c\mathbf{p}_{o,1}) - \left(({}^c\mathbf{p}_{o,2} - {}^c\mathbf{p}_{o,1})^T {}^c\mathbf{n} \right) {}^c\mathbf{n} \\ {}^c\hat{\mathbf{y}} &= \frac{{}^c\mathbf{y}}{\|{}^c\mathbf{y}\|} \\ {}^c\hat{\mathbf{z}} &= {}^c\hat{\mathbf{x}} \times {}^c\hat{\mathbf{y}} \end{aligned} \tag{51}$$

Let

$$\begin{aligned} {}^r\mathbf{M}_3 &= \begin{bmatrix} {}^r\hat{\mathbf{x}} & {}^r\hat{\mathbf{y}} & {}^r\hat{\mathbf{z}} \end{bmatrix} \\ {}^c\mathbf{M}_3 &= \begin{bmatrix} {}^c\hat{\mathbf{x}} & {}^c\hat{\mathbf{y}} & {}^c\hat{\mathbf{z}} \end{bmatrix} \end{aligned} \tag{52}$$

Then the rotation $\mathbf{R}_{cr}$ and translation $\mathbf{t}_{cr}$ can be computed as

$$\begin{aligned} \mathbf{R}_{cr} &= {}^{c}\mathbf{M}_3 {}^{r}\mathbf{M}_3^T \\ \mathbf{t}_{cr} &= {}^{c}\mathbf{p}_{o,1} - \mathbf{R}_{cr} {}^{r}\mathbf{p}_{o,1} \end{aligned} \tag{53}$$

6 previous version

6.1 Points' Constraints on Camera Motion

Suppose that all the occluding edge points are directly used in the pose estimation.

$$\begin{aligned} J_p(\mathbf{w}) &= \sum_{k=1}^{N_p} J_{p,k} = \sum_{k=1}^{N_p} \mathbf{e}_k^T \mathbf{e}_k \\ &= \sum_{k=1}^{N_p} \left({}^{c}\mathbf{p}'_{o,k} - R_{cr}\left({}^{r}\mathbf{p}'_{o,k}\right) - \mathbf{t}'_{cr}\right)^T \left({}^{c}\mathbf{p}'_{o,k} - R_{cr}\left({}^{r}\mathbf{p}'_{o,k}\right) - \mathbf{t}'_{cr}\right)) \end{aligned} \tag{54}$$

where all the point coordinates are referred to the centroid.

$$\begin{aligned} &\mathbf{t}'_{cr} = \mathbf{t}_{cr} - {}^{c}\bar{\mathbf{p}}_o + R_{cr}({}^{r}\bar{\mathbf{p}}_o) \\ &{}^{c}\mathbf{p}'_{o,k} = {}^{c}\mathbf{p}_{o,k} - {}^{c}\bar{\mathbf{p}}_o,\ {}^{r}\mathbf{p}'_{o,k} = {}^{r}\mathbf{p}_{o,k} - {}^{r}\bar{\mathbf{p}}_o \\ &{}^{c}\bar{\mathbf{p}}_o = \frac{1}{N_p}\sum_{k=1}^{N_p} {}^{c}\mathbf{p}_{o,k},\ {}^{r}\bar{\mathbf{p}}_o = \frac{1}{N_p}\sum_{k=1}^{N_p} {}^{r}\mathbf{p}_{o,k} \end{aligned} \tag{55}$$

The scatter matrix $\mathbf{\Psi}_p$ is defined likewise.

$$\mathbf{\Psi}_p = \sum_{k=1}^{N_p} \left(\frac{\partial J_{p,k}}{\partial \mathbf{w}}\right) \left(\frac{\partial J_{p,k}}{\partial \mathbf{w}}\right)^T \tag{56}$$

where

$$\frac{\partial J_{p,k}}{\partial \mathbf{w}} = -2 \begin{bmatrix} \mathbf{I}_{3\times 3} \\ {}^{r}\hat{\mathbf{p}}'_{o,k} \end{bmatrix} \left({}^{c}\mathbf{p}'_{o,k} - R_{cr}({}^{r}\mathbf{p}'_{o,k}) - \mathbf{t}_{cr}\right) \tag{57}$$

6.2 Degenerate Cases

(1) It can be seen from $\mathbf{\Psi}_p$ that if $\exists \mathbf{v}$ such that ${}^{r}\mathbf{p}'_{o,k} \times \mathbf{v} = 0$ for all $k = 1, \cdots, N_p$, i.e., the measured points are collinear (at least two points), $\delta J_p(\delta\mathbf{w}) = \delta\mathbf{w}^T \mathbf{\Psi}_p \delta\mathbf{w} = 0$ for $\delta\mathbf{w} = [\mathbf{0}^T, \mu\mathbf{v}^T]^T$.

(2) If there is only one measured point, ${}^{r}\mathbf{p}'_{o,k} = \mathbf{0}$. In this case, for any rotation $\omega \in \mathbb{R}^3$, $\delta J_p(\delta\mathbf{w}) = \delta\mathbf{w}^T \mathbf{\Psi}_p \delta\mathbf{w} = 0$ for $\delta\mathbf{w} = [\mathbf{0}^T, \omega^T]^T$.

6.2.1 Point Weighting

For each occluding edge point ${}^{c}\mathbf{p}_{o,k}$, a weight $\alpha_{p,k}$ is assigned to the corresponding component in the cost function

$$J_{pw}(\mathbf{w}) = \sum_{k=1}^{N_p} \alpha_{p,k} J_{p,k} \tag{58}$$

$$\alpha_{p,k} = \frac{\left(\frac{\partial J_{p,k}}{\partial \mathbf{w}}\right)^T \mathbf{q}_{\pi,j}}{\left|\frac{\partial J_{p,k}}{\partial \mathbf{w}}\right| \sqrt{\frac{\lambda_{\pi,j}}{\bar{\lambda}_\pi}}} \tag{59}$$

$$j = \arg\max_j \frac{\left(\frac{\partial J_{p,k}}{\partial \mathbf{w}}\right)^T \mathbf{q}_{\pi,j}}{\left|\frac{\partial J_{p,k}}{\partial \mathbf{w}}\right|} \tag{60}$$

$$\bar{\lambda}_\pi = \frac{1}{6}\sum_{t=1}^{6} \lambda_{\pi,t} \tag{61}$$

6.2.2 Degenerate Cases

Suppose that the measurements include both planes and points. Combining the degenerate cases stated in 1.1.2 and 1.2.2 yields the following cases.

(1) $\lambda_{\pi,1} = \lambda_{\pi,2} = 0$ and ${}^r\mathbf{p}'_{o,k} \times \mathbf{v} = 0$ for all $k = 1, \cdots, N_p$ hold true simultaneously, and $\mathbf{v}$ and $\mathbf{v}_{\pi,1}$ happen to be of the same direction, i.e., $\mathbf{v} \times \mathbf{v}_{\pi,1} = 0$. In this case, the camera motion along $\delta\mathbf{w} = [\mathbf{0}^T, \mu\mathbf{v}_{\pi,1}^T]^T$ cannot be constrained.

(2) If $\lambda_{\pi,1} = \lambda_{\pi,2} = 0$ and there is only one measured point, the camera motion along $\delta\mathbf{w} = [\mathbf{0}^T, \mu\mathbf{v}_{\pi,1}^T]^T$ cannot be constrained.

7 Plane and Point based Camera Tracking with Unknown Correspondences

The plane segmentation method proposed in [1] and the edge detection method proposed in [2] are used to detect the planar segments and edge points in an RGB-D scan.

A detected planar segment $\mathcal{P}_i, i = 1, \cdots, N$ has the following attributes.

- plane parameters $\pi_i = [\mathbf{n}_i^T, d_i]^T$
- number of points $N_{\pi,i}$
- centroid $\mathbf{p}_{\pi,i}$
- covariance $\mathbf{C}_{\pi,i}$

Suppose that $\{{}^r\mathcal{P}_i\}_{i=1,\cdots,N_r}$ and $\{{}^c\mathcal{P}_j\}_{j=1,\cdots,N_c}$ are planar segments extracted from reference and current frame, respectively. Each planar segment $\mathcal{P}_i$ is modeled as a Gaussian distribution $\mathcal{N}(\mathbf{p}_{\pi,i}, \mathbf{C}_{\pi,i})$. $\{{}^r\mathbf{p}_{o,k}\}_{k=1,\cdots,N_{pr}}$ and $\{{}^c\mathbf{p}_{o,l}\}_{l=1,\cdots,N_{pc}}$ are occluding edge points extracted from reference and current frame, respectively. The planar segments and occluding edge points extracted from two successive frames are used simultaneously in a ICP framework. In each iteration of ICP, the correspondences between planar segments are assigned by checking the Bhattacharyya distance between the Gaussian distribution that models the planar segments.

$$D_{Bha}(\mathcal{P}_i, \mathcal{P}_j) = \frac{1}{8}(\mathbf{p}_{\pi,i} - \mathbf{p}_{\pi,j})^T \mathbf{C}_\pi^{-1} (\mathbf{p}_{\pi,i} - \mathbf{p}_{\pi,j}) + \frac{1}{2}\ln\left(\frac{|\mathbf{C}_\pi|}{\sqrt{|\mathbf{C}_{\pi,i}||\mathbf{C}_{\pi,j}|}}\right) \tag{62}$$

Table 2:

	Plane-Point ICP	STING
Fr1/xyz	0.0123	**0.0114**
Fr1/room	**0.0817**	0.0832
Fr3/cabinet	0.0382	**0.0326**

where $\mathbf{C}_\pi = \frac{1}{2}\left(\mathbf{C}_{\pi,i} + \mathbf{C}_{\pi,j}\right)$. The correspondences between points are assigned by checking the Euclidean distance between the point coordinates.

$$D_{Euc}(\mathbf{p}_{o,k}, \mathbf{p}_{o,l}) = \|\mathbf{p}_{o,k} - \mathbf{p}_{o,l}\|_2 \tag{63}$$

The whole ICP framework is presented in Algorithm 2.

Algorithm 2 Planar Segment and Occluding Edge Point based ICP

Inputs:

Planar segments extracted from two frames $\{{}^r\mathcal{P}_i\}_{i=1,\cdots,N_r}$ and $\{{}^c\mathcal{P}_j\}_{j=1,\cdots,N_c}$.

Occluding edge points extracted from two frames $\{{}^r\mathbf{p}_{o,k}\}_{k=1,\cdots,N_{pr}}$ and $\{{}^c\mathbf{p}_{o,l}\}_{l=1,\cdots,N_{pc}}$.

Outputs:

Transformation between two frames $T_{cr} = \mathbf{R}_{cr}, \mathbf{t}_{cr}$.

8 Plane Fusion

A plane $\mathcal{P}_i$

- plane parameters $\pi_i = [\mathbf{n}_i^T, d_i]^T$
- number of points $N_{\pi,i}$
- centroid $\mathbf{p}_{\pi,i}$
- covariance $\mathbf{C}_{\pi,i}$
- curvature $\rho_{\pi,i}$ [2]
- shadow points $\left\{\mathbf{p}_{s,k}^i, k = 1, \cdots, N_p^i\right\}$

9 Least Primitives for Pose Estimation

9.1 Three Planes

Three corresponding non-parallel planes $\{{}^r\pi_i, {}^c\pi_i, \}_{i=1,2,3}$. Let

$$\begin{aligned} {}^r\mathbf{M}_1 &= \begin{bmatrix} {}^r\mathbf{n}_1 & {}^r\mathbf{n}_2 & {}^r\mathbf{n}_3 \end{bmatrix} \\ {}^c\mathbf{M}_1 &= \begin{bmatrix} {}^c\mathbf{n}_1 & {}^c\mathbf{n}_2 & {}^c\mathbf{n}_3 \end{bmatrix} \\ \mathbf{d} &= \begin{bmatrix} {}^cd_1 - {}^rd_1 \\ {}^cd_2 - {}^rd_2 \\ {}^cd_3 - {}^rd_3 \end{bmatrix} \end{aligned} \tag{64}$$

[2]Note that the curvature here is just an indication that tells how a surface deviates from being a flat plane, rather than the strictly defined curvature.

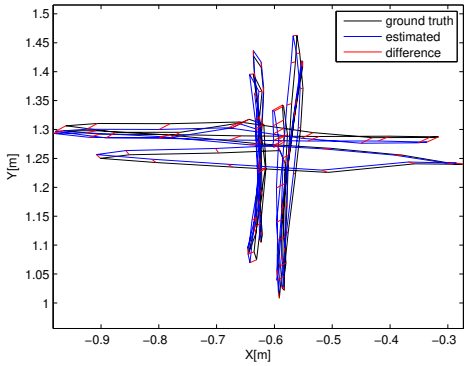

(a)

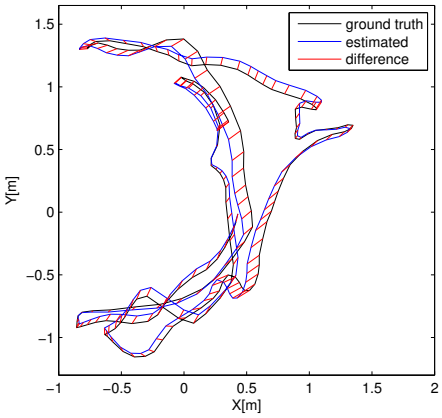

(b)

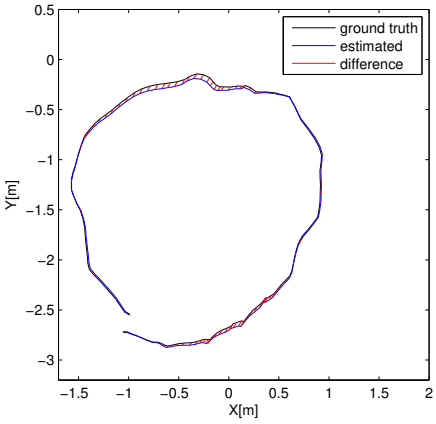

(c)

Figure 6: (a)Fr1/xyz; (b)Fr1/room; (c)Fr3/cabinet;

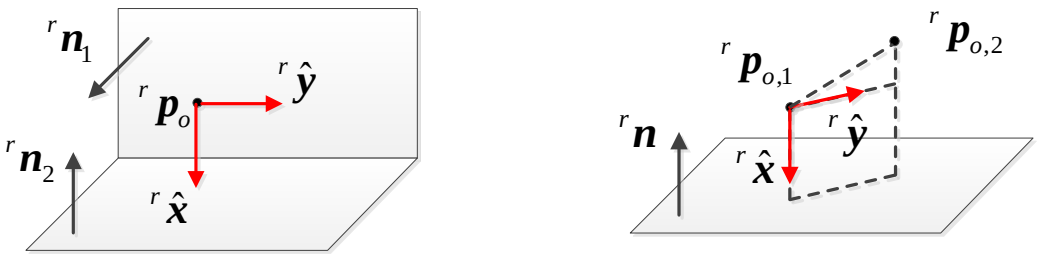

(a) (b)

Figure 7:

The rotation $\mathbf{R}_{cr}$ and translation $\mathbf{t}_{cr}$ can be computed as

$$\begin{aligned} \mathbf{R}_{cr} &= {}^c\mathbf{M}_1 {}^r\mathbf{M}_1^{-1} \\ \mathbf{t}_{cr} &= {}^c\mathbf{M}_1^{-T}\mathbf{d} \end{aligned} \tag{65}$$

9.2 Two Planes and One Point

Two corresponding non-parallel planes $\{{}^r\pi_i, {}^c\pi_i,\}_{i=1,2}$ and one corresponding point $\{{}^r\mathbf{p}_o, {}^c\mathbf{p}_o\}$. Construct three axes ${}^r\hat{\mathbf{x}}, {}^r\hat{\mathbf{y}}, {}^r\hat{\mathbf{z}}$ in reference coordinate system and locate the origin at ${}^r\mathbf{p}_o$.

$$\begin{aligned} {}^r\hat{\mathbf{x}} &= -{}^r\mathbf{n}_2 \\ {}^r\hat{\mathbf{y}} &= {}^r\mathbf{n}_1 \times {}^r\mathbf{n}_2 \\ {}^r\hat{\mathbf{z}} &= {}^r\hat{\mathbf{x}} \times {}^r\hat{\mathbf{y}} \end{aligned} \tag{66}$$

The axes and the origin in current frame is constructed likewise.

$$\begin{aligned} {}^c\hat{\mathbf{x}} &= -{}^c\mathbf{n}_2 \\ {}^c\hat{\mathbf{y}} &= {}^c\mathbf{n}_1 \times {}^c\mathbf{n}_2 \\ {}^c\hat{\mathbf{z}} &= {}^c\hat{\mathbf{x}} \times {}^c\hat{\mathbf{y}} \end{aligned} \tag{67}$$

Let

$$\begin{aligned} {}^r\mathbf{M}_2 &= \begin{bmatrix} {}^r\hat{\mathbf{x}} & {}^r\hat{\mathbf{y}} & {}^r\hat{\mathbf{z}} \end{bmatrix} \\ {}^c\mathbf{M}_2 &= \begin{bmatrix} {}^c\hat{\mathbf{x}} & {}^c\hat{\mathbf{y}} & {}^c\hat{\mathbf{z}} \end{bmatrix} \end{aligned} \tag{68}$$

Then the rotation $\mathbf{R}_{cr}$ and translation $\mathbf{t}_{cr}$ can be computed as

$$\begin{aligned} \mathbf{R}_{cr} &= {}^c\mathbf{M}_2 {}^r\mathbf{M}_2^T \\ \mathbf{t}_{cr} &= {}^c\mathbf{p}_o - \mathbf{R}_{cr} {}^r\mathbf{p}_o \end{aligned} \tag{69}$$

9.3 One Plane and Two Points

One corresponding plane $\{{}^r\pi, {}^c\pi,\}$ and two different corresponding points $\{{}^r\mathbf{p}_{o,j}, {}^c\mathbf{p}_{o,j}\}_{j=1,2}$ satisfying $({}^r\mathbf{p}_{o,1} - {}^r\mathbf{p}_{o,2}) \times {}^r\mathbf{n} \neq 0$ and $({}^c\mathbf{p}_{o,1} - {}^c\mathbf{p}_{o,2}) \times {}^c\mathbf{n} \neq 0$. Construct three axes ${}^r\hat{\mathbf{x}}, {}^r\hat{\mathbf{y}}, {}^r\hat{\mathbf{z}}$ in reference coordinate system and locate the origin at ${}^r\mathbf{p}_{o,1}$.

$$\begin{aligned} {}^r\hat{\mathbf{x}} &= -{}^r\mathbf{n} \\ {}^r\mathbf{y} &= ({}^r\mathbf{p}_{o,2} - {}^r\mathbf{p}_{o,1}) - \left(({}^r\mathbf{p}_{o,2} - {}^r\mathbf{p}_{o,1})^T {}^r\mathbf{n}\right) {}^r\mathbf{n} \\ {}^r\hat{\mathbf{y}} &= \frac{{}^r\mathbf{y}}{\|{}^r\mathbf{y}\|} \\ {}^r\hat{\mathbf{z}} &= {}^r\hat{\mathbf{x}} \times {}^r\hat{\mathbf{y}} \end{aligned} \tag{70}$$

The axes and the origin in current frame is constructed likewise.

$$
\begin{aligned}
{}^{c}\hat{\mathbf{x}} &= -{}^{c}\mathbf{n} \\
{}^{c}\mathbf{y} &= ({}^{c}\mathbf{p}_{o,2} - {}^{c}\mathbf{p}_{o,1}) - \left(({}^{c}\mathbf{p}_{o,2} - {}^{c}\mathbf{p}_{o,1})^{T}\, {}^{c}\mathbf{n}\right) {}^{c}\mathbf{n} \\
{}^{c}\hat{\mathbf{y}} &= \frac{{}^{c}\mathbf{y}}{\|{}^{c}\mathbf{y}\|} \\
{}^{c}\hat{\mathbf{z}} &= {}^{c}\hat{\mathbf{x}} \times {}^{c}\hat{\mathbf{y}}
\end{aligned}
\tag{71}
$$

Let

$$
\begin{aligned}
{}^{r}\mathbf{M}_3 &= \begin{bmatrix} {}^{r}\hat{\mathbf{x}} & {}^{r}\hat{\mathbf{y}} & {}^{r}\hat{\mathbf{z}} \end{bmatrix} \\
{}^{c}\mathbf{M}_3 &= \begin{bmatrix} {}^{c}\hat{\mathbf{x}} & {}^{c}\hat{\mathbf{y}} & {}^{c}\hat{\mathbf{z}} \end{bmatrix}
\end{aligned}
\tag{72}
$$

Then the rotation $\mathbf{R}_{cr}$ and translation $\mathbf{t}_{cr}$ can be computed as

$$
\begin{aligned}
\mathbf{R}_{cr} &= {}^{c}\mathbf{M}_3 {}^{r}\mathbf{M}_3^{T} \\
\mathbf{t}_{cr} &= {}^{c}\mathbf{p}_{o,1} - \mathbf{R}_{cr} {}^{r}\mathbf{p}_{o,1}
\end{aligned}
\tag{73}
$$

References

[1] Efficient Organized Point Cloud Segmentation with Connected Components, SPME, 2013.

[2] RGB-D Edge Detection and Edge-based Registration, IROS, 2013.

[3] K. Khoshelham and S. O. Elberink, "Accuracy and resolution of Kinect depth data for indoor mapping applications," Sensors, vol. 12, no. 2, pp. 1437-1454, 2012.